archives
of thermodynamics
Vol. **41**(2020), No. 2, 257–276
DOI: 10.24425/ather.2020.133632

Experimental investigation of gravity-assisted wickless heat pipes (thermosyphons) at low heat inputs for solar application

HASSAN NAJI SALMAN AL-JOBOORY*

Renewable Energy Directorate, Ministry of Science and Technology, Karrada, Al-Jaderiyah, Baghdad, Iraq

Abstract The performance of ten wickless heat pipes without adiabatic sections is investigated experimentally at low heat inputs 120 to 2000 W/m^2 for use in solar water heaters. Three heat pipe diameter groups were tested, namely 16, 22, and 28.5 mm. Each group had evaporator lengths of 1150, 1300, and 1550 mm, respectively, with an extra evaporator length of 1800 mm added to the second group. The condenser section length of all heat pipes was 200 mm. Ethanol, methanol, and acetone were utilized as working fluids, at inventory of 25%, 50%, 70%, and 90% by evaporator volume respectively. The 22 mm diameter pipes were tested at inclination angles 30°, 45°, and 60°. Other diameter groups were tested at 45° only. Experiments revealed increased surface temperatures and heat transfer coefficients with increased pipe diameter and evaporator length, and that increased working fluid inventory caused pronounced reduction in evaporator surface temperature accompanied by improved heat transfer coefficient to reach maximum values at 50% inventory for the selected fluids. Violent noisy shocks were observed with 70% and 90% inventories with the tested heat pipes and the selected working fluids with heat flux inputs from 320–1900 W/m^2. These shocks significantly affected the heat pipes heat transfer capability and operation stability. Experiments revealed a 45° and 50% optimum inclination angle of fill charge ratio respectively, and that wickless heat pipes can be satisfactorily used in solar applications. The effect of evaporator length and heat pipe diameter on the performance was included in data correlations.

Keywords: Wickless heat pipe; Adiabatic section; Solar heat pipe; Fill charge ratio; Working fluid inventory; Inclination angle

*E-mail: haljoboory@gmail.com

Nomenclature

A – surface area, m^2
B – coefficient of thermal expansion, K^{-1}
C – constant
c_p – specific heat capacity, kJ/(kg K)
d – heat pipe diameter, m
FR – working fluid fill charge ratio based on evaporator volume, %
g – gravitational acceleration, m/s^2
Gr – Grashof number, $= gB\rho^2 l_m^3 \Delta T_{ev}/\mu^2$
h – heat transfer coefficient, $W/(m^2K)$
I – electrical current, A
k – thermal conductivity, W/(m K)
L_{ev} – evaporator section length, m
L_{co} – condenser section length, m
l_m – characteristic bubble length scale, m
Nu – Nusselt number, $= hl_m/k_l$
n – exponent, constant
P – input electric power, W
Pr – Prandtle number $= c_p\mu/k$
Q – heat rate, W
q – heat flux, $= Q/A$, W/m^2
Ra – Raleigh number, = GrPr
Re – Reynolds number, $= \rho ud/\mu$
Re_m – modified Reynolds number, $= ReL_{ev}/d$
T – temperature, K
U – voltage, V
$\dot{V}$ – volumetric flow rate, m^3/s

Greek symbols

β – inclination angle, °
Δ – difference
ε – emissivity
ρ – density, kg/m^3
σ – Stefan-Boltzman constant, W/ m^2K^4
μ – dynamic viscosity, N/ms

Subscripts

a – ambient
$conv$ – convection
$corr$ – correlation
ev – evaporator
rad – radiation
v – vapor
w – water

1 Introduction

The performance of heat pipes is governed by many parameters such as working fluid type and inventory, orientation, geometry, materials, and wick structure. Selection of heat pipe working fluid and materials is determined by the operating conditions particularly the operating temperature and heat input. Heat pipes for solar applications operate at temperatures near 100 °C or lower.

The amount of working fluid (fill charge ratio, inventory) charged into the heat pipe is one of the essential parameters that determines the operation and performance of heat pipes, as was observed by Jiao *et al.* [1]. Larkin established that the maximum heat transportability of heat pipes increased with increasing fill charge ratio [2]. Ristoiu *et al.* [3] also concluded that, for inclined wickless heat pipes using alcohol, acetone and water as working fluids, the range of isothermal operation depends deeply on the working fluid fill charge. The effect of different working fluid types and inventories on the heat pipe performance was investigated by many researches [2–7,8–11]. An optimum fill charge ratio in the range of 25–90% has been reported, these values for wickless heat pipes operating at low heat fluxes are, however, limited.

A range of inclinations exists at which heat pipes show better performance than the vertical position. Sheraishi *et al.* [4,5] reported optimum inclination angles of 40°–50° from the horizontal. Negishi and Sawada recommended an inclination between 20° and 40° for water, and more than 5° for ethanol [6]. Mahdy recommended an optimum range of 30°–60° for evaporator-wicked heat pipes [7]. A similar result was reported by Witwit [8], Hahn and Gross [9], and others [8–12].

The heat transfer coefficient for natural convection regime inside the heat pipe is usually correlated by the standard expression

$$\mathrm{Nu} = C(\mathrm{GrPr})^n = C\mathrm{Ra}^n \ . \tag{1}$$

Several modifications have been proposed by various investigators such as El-Genk and Saber [15,16], Imura *et al.* [17] and others [13,18–22]. Mahdy presented a correlation for water, ethanol and R-113 charged evaporator-wicked heat pipes in the following form[7]:

$$\mathrm{Nu} = f(\mathrm{Re}_m, \mathrm{Gr}, f(\beta)) \ , \tag{2}$$

where Re_m is a modified Reynolds number, obtained by multiplying the Reynolds number by the dimensionless length ratio (L_{ev}/L_{co}) which was

introduced to account for variations in the evaporator length. The factor $f(\beta)$ that accounts for the effect of inclination angle (β) was given as

$$f(\beta) = \left(\frac{\beta}{180} + \sqrt{\sin 2\beta}\right)^{0.65} . \tag{3}$$

Most empirical correlations agree only with the experimental data they correlate. No correlation was found that includes the effect of heat pipe evaporator length and diameter at low heat inputs.

This work investigates the performance of wickless heat pipes at low heat inputs that may be encountered in solar applications, especially solar water heaters incorporating flat plate and evacuated tube solar collectors where heat pipes can be used as heat transfer conductors from the heat source (solar absorber) towards the heat sink (storage water). New correlations were formulated that include the effect of heat pipe evaporator length and diameter in a dimensionless ratio defined as L_{ev}/d.

2 Heat pipe manufacture

The heat pipe containers were made of standard copper tubes of 16 mm, 22 mm, and 28.5 mm outside diameters. Table 1 shows the heat pipe characteristics and the experimental program. The end caps were fabricated from copper. A 3 mm hole was drilled at the center of the cap on the evaporator end to provide access for the heat pipe core temperature measurement probe. Two other 3 mm holes were drilled in the cap on the condenser end, one for the temperature probe and the other for the charging tube. The temperature of the liquid and vapor in the interior space of the heat pipe was measured by passing the thermocouples through two 3 mm copper tubes. Thermocouple beads were then allowed to protrude through 1 mm holes drilled at specified placements through the probe to the heat pipe core. The probes, charging tubes and charging valves were fixed at the end caps by brazing. Heat pipe components were cleaned thoroughly and then assembled and brazed. The heat pipes were evacuated by a vacuum pump rated at an absolute pressure 1.33 Pa with simultaneous gradual heating to temperatures above 102 °C to remove the free and adsorbed gas molecules from the heat pipe internal surfaces. All heat pipes were vacuum-tested at 1.33 Pa for 48 hours and then charged with the specified amount of the working fluid. Incorporation of a heat pipe as thermal conductors in a solar system is achieved by integrating the evaporator section into the solar

collector to absorb the collected solar energy, while the condenser section protrudes into the heat sink (storage tank or manifold). The heat pipe working fluid works as the heat transfer medium.

Table 1: Heat pipe characteristics.

Heat Pipe	Group 1			Group 2				Group 3		
Type	wickless			wickless				wickless		
Material	copper			copper				copper		
Code	HP1	HP2	HP3	HP4	HP5	HP6	HP7	HP8	HP9	HP10
Evaporator length (mm)	1150	1300	1550	1150	1300	1550	1800	1150	1300	1550
Diameter (mm)	16			22				28.5		
Condenser length (mm)	200			200				200		
Adiabatic length (mm)	0			0				0		
Working fluid	ethanol, methanol, acetone			ethanol, methanol, acetone				ethanol, methanol, acetone		
Fill charge ratio (%)	25, 50, 70, 90			25, 50, 70, 90				25, 50, 70, 90		
Inclination angle (°)	45			30, 45, 60				45		
Heat input (W)	10–235			10–235				10–235		

3 The experimental apparatus

The experimental apparatus with instrumentation is shown schematically in Fig. 1. The heat pipe evaporator is heated by a 0.5 mm diameter Ni-Cr non magnetic resistance heating wire passed through ceramic beads. Two layers of asbestos cloth were wrapped, one on the evaporator wall before wrapping the electric heater, and the other is wrapped on the heater. A 50 mm thick glass wool insulation was wrapped to ensure minimum heat losses to the surroundings and one-dimensional heat flow. The heating wire terminals were connected to a variable transformer, through a power stabilizer. The power was measured by digital voltmeter and ammeter connected to its terminals. A 50 mm diameter plastic jacket, insulated by 10 mm thick armaflex rubber insulation and wrapped by 20 mm thick glass wool

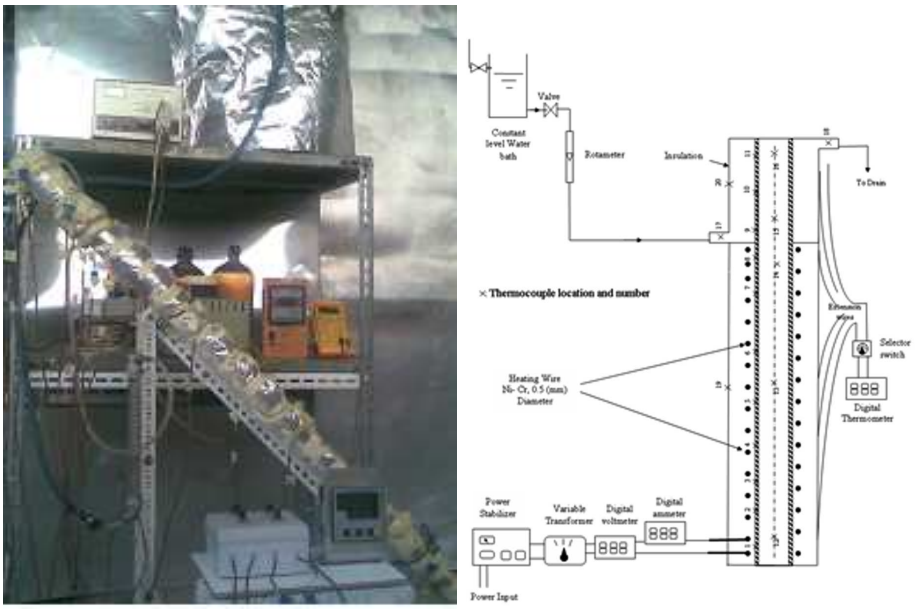

Figure 1: Experimental heat pipe test rig with instrumentation.

insulation, was used at the heat pipe condenser section for cooling water flow. In order to measure the temperatures at specified locations (heat pipe outer surface and inner space, insulation surfaces, cooling water temperature at inlet and outlet, surrounding ambient), 0.2 mm calibrated copper-constantan thermocouples were used. The thermocouples were distributed around the circumference of the heat pipe outer surfaces at the evaporator and condenser sections to measure the circumferential temperature. The heat transport by the heat pipe to the cooling water was obtained by

$$Q_w = \rho_w \dot{V} c_p \Delta T \ . \tag{4}$$

The cooling water discharge was measured by 0.1 l/h accuracy rotameter. The power input was calculated by the equation

$$P = IU \ . \tag{5}$$

The heat loss for the worst case was approximately 1.5 W (14.3%) at low heat inputs, and 28.4 W (12.1%) at maximum heat input. The net heating power applied into the evaporator section was calculated from

$$Q_{net} = P - (Q_{conv} + Q_{rad})_{loss} \ . \tag{6}$$

An energy balance was conducted to check the accuracy of measurements as follows:

$$Q_{net} = Q_w + (Q_{conv} + Q_{rad})_{loss} , \tag{7}$$

where

$$Q_{conv} = h_{conv} A (T_{surface} - T_a) \tag{8}$$

and

$$Q_{rad} = \sigma \varepsilon A (T_{surface-T_a}) . \tag{9}$$

The cooling water flow rate and inlet temperature were kept constant at 6 l/h and 23 ±2 °C throughout the experiments. Measurements were carried out at steady state conditions when each thermocouple reading was within no more than ±2 °C fluctuation.

4 Results and discussion

Figure 2 illustrates typical wall temperature distribution along the outer surface for heat pipe HP7 under various heat inputs with ethanol as the working fluid. The results for HP7 are shown as typical for the other

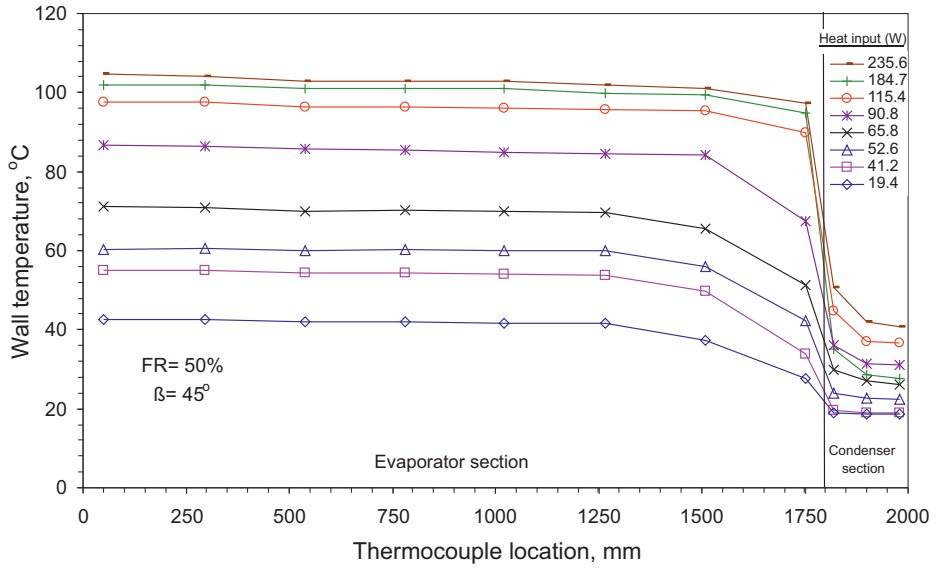

Figure 2: Wall temperature distribution for heat pipe HP7 with ethanol.

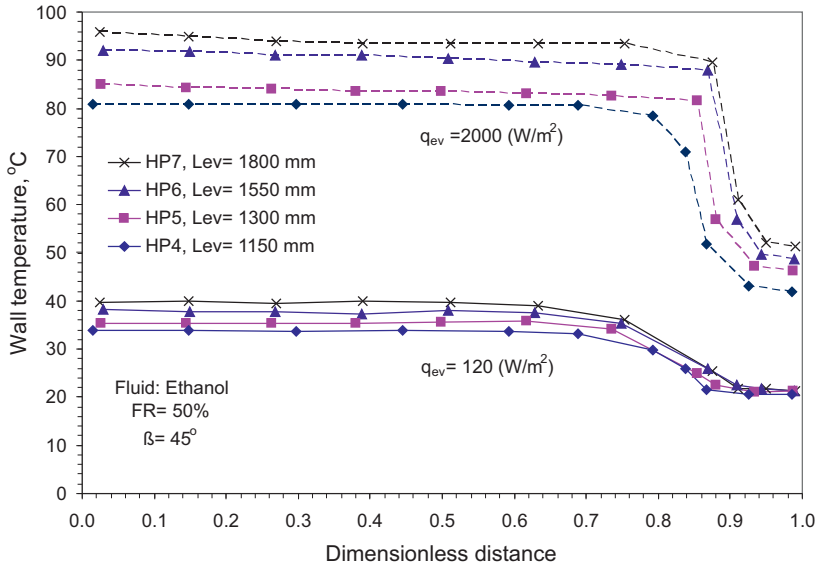

Figure 3: Effect of evaporator length (at 22 mm diameter) on the heat pipe wall temperature distribution.

heat pipes. The evaporator surface temperature behavior was observed to be almost isothermal, since there exists a continuous condensate film layer covering the inner evaporator surface, the heat pipe wall temperature rises with increased heat input for all tested heat pipes. At the evaporator-condenser interface, the surface temperature gradient dropped steeply before becoming isothermal again along the rest of the condenser section, such a behavior was expected due to the absence of an adiabatic section. Typical results for the wall temperature distribution with varying heat pipe evaporator lengths are shown in Fig. 3. Pipe diameters in this figure are all equal and for a low heat flux of 120 W/m^2 and a high heat flux of 2000 W/m^2 with ethanol as the working fluid at 50% fill charge ratio and 45° inclination angle. The dimensionless distance of the abscissa is defined as the thermocouple position divided by the total heat pipe length. The wall temperature is higher for the longer evaporator length. The average temperature difference between the shorter and longer heat pipes was within 4 °C at low heat flux and was up to 13 °C at high heat flux. Another typical effect of heat pipe diameter, for equal evaporator lengths, on the wall temperature distribution is shown in Fig. 4 at a low heat flux of

120 W/m^2 and a high heat flux of 2000 W/m^2 with ethanol at 50% fill charge ratio and 45° inclination angle. A larger diameter heat pipe operates at a higher wall temperature. An average difference of nearly 6 °C is noticed at low heat flux which increases to a difference of up to 18 °C at high heat flux.

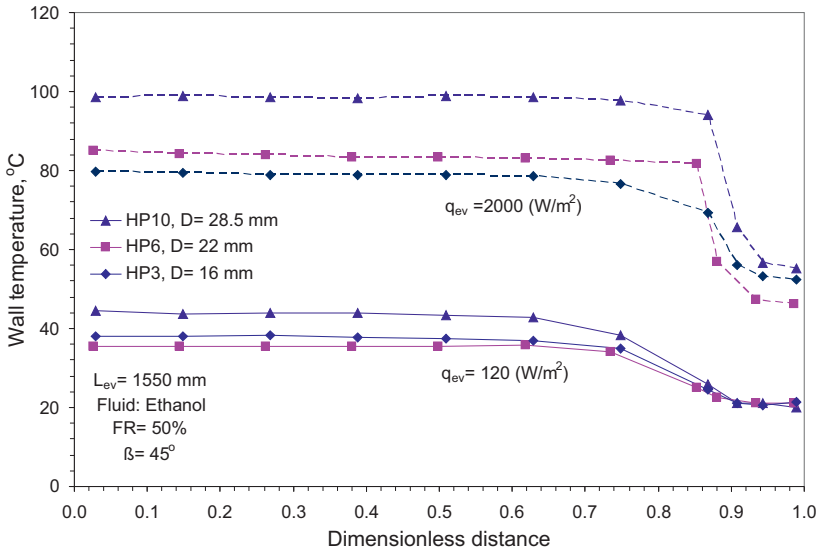

Figure 4: Effect of heat pipe diameter (at 1550 mm evaporator length) on the heat pipe wall temperature distribution.

Figure 5 shows the wall temperature distribution for the three working fluids. Methanol heat pipe operates at the lowest temperature. The difference in mean evaporator temperature behavior is insignificant at low heat inputs. However, as the heat flux input is increased, the difference becomes more significant. Moreover, slightly lower evaporator temperatures were observed with heat pipes charged with methanol than acetone and ethanol. A similar trend was observed for the rest of heat pipes. This reveals the possibility to utilize various heat pipe working fluids in the solar applications.

The effect inclination angle of heat pipes on the wall temperature distribution is shown in Fig. 6 for ethanol charged heat pipe HP7 at low and high heat inputs. A slight difference in the mean evaporator temperature is observed at high heat inputs, a difference that is typical for the other test fluids.

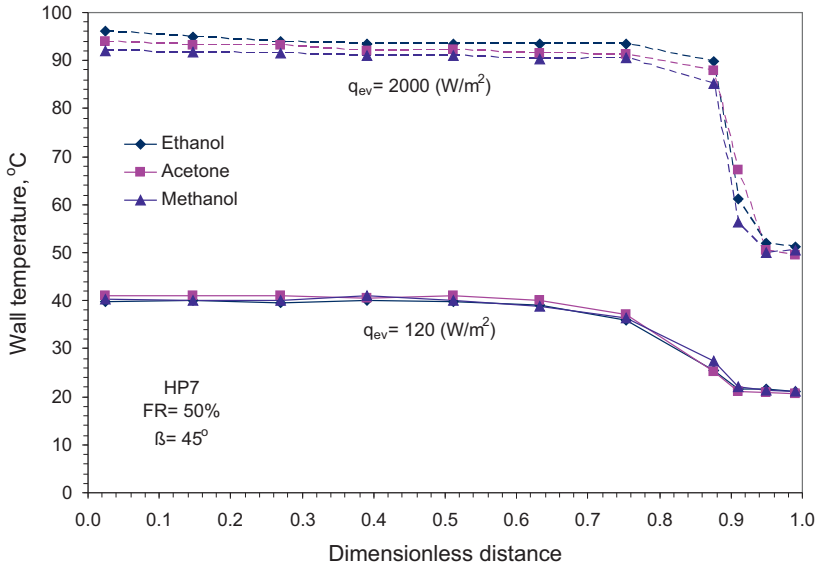

Figure 5: Effect of heat pipe working fluid on the wall temperature distribution.

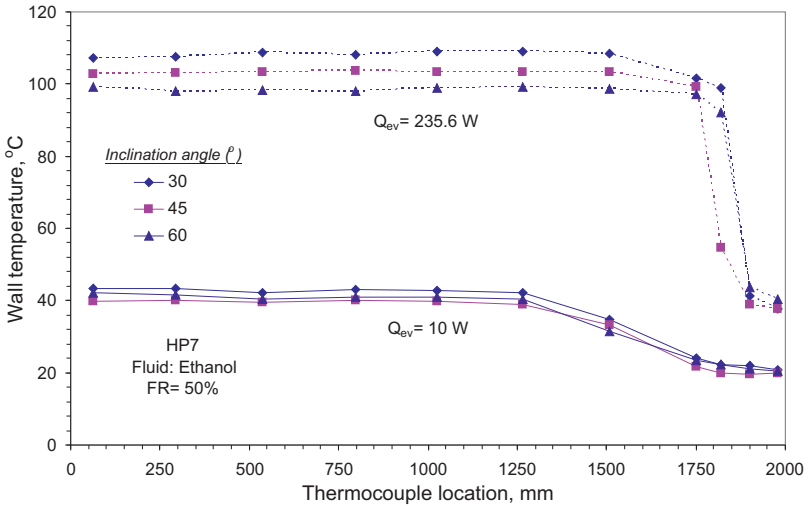

Figure 6: Effect of inclination angle on the heat pipe wall temperature distribution.

Figure 7 shows the effect of fill charge ratio on the wall temperature distribution for heat pipe HP7 for ethanol as typical for the other fluids. The

inclination angle is 45° and heat inputs are 10 W and 235.6 W. At low heat inputs the difference of the in temperature variation between the four test fluid inventories did not exceed 2 °C. This result is also true for the other heat pipes. As heat inputs increased to high values, however, the effect of fluid inventory becomes more significant for the three tested working fluids where the temperature variation was observed to vary by 2 °C to 14 °C, depending on the working fluid type and inventory. As a result, lower evaporator surface temperature is induced with increased working fluid inventory (fill charge ratio).

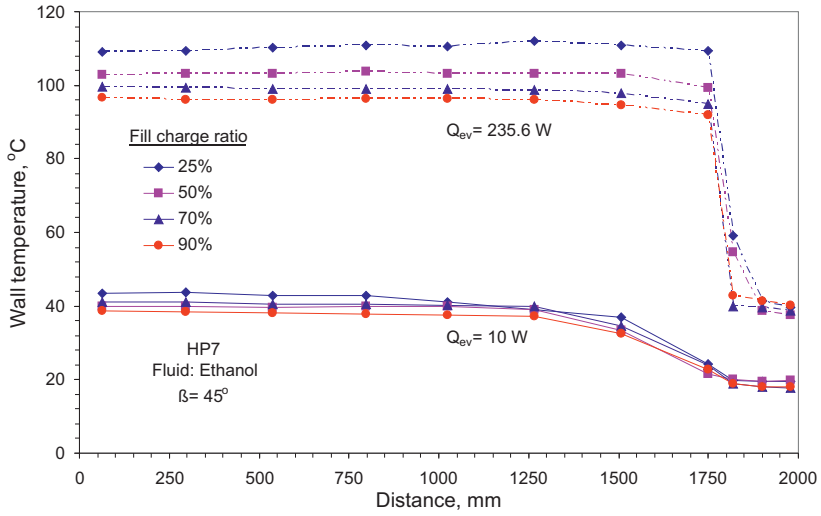

Figure 7: Effect of the working fluid inventory on the heat pipe wall temperature distribution.

The effect of fluid inventory at the three test working fluids on the mean evaporator temperature shown in Fig. 8. Methanol charged heat pipes have lower operating temperature than those charged with ethanol and acetone, the operating temperatures decrease with increased fluid inventories by 12 °C for ethanol, 9 °C for acetone, and 15 °C for methanol. A phenomenon was observed clearly at a range of heat input values from 40 W to 110 W and fill charge ratios of 70% and 90%, a repeated periodical strange bang inside the heat pipe container was heard and accompanied with a sudden violent shock of the test heat pipe, followed by a sudden drop in the evaporator temperature. The time of the period of this phenomenon was within of

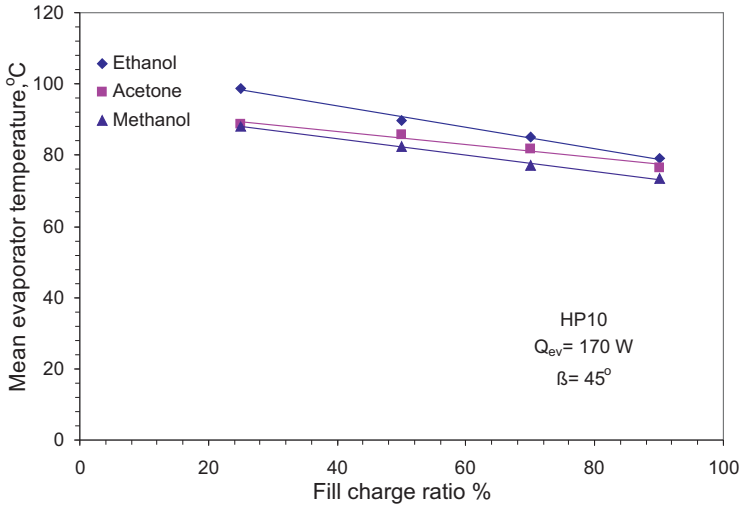

Figure 8: Effect of the fill charge ratio with various working fluids on the operating temperature.

1–2 min for the 90% fill charged heat pipes, and within 4–5 min for the 70% fill charged heat pipes. A typical effect of this phenomenon is shown in Fig. 9 for heat pipe HP3 with methanol at 70% fill charge ratio. This

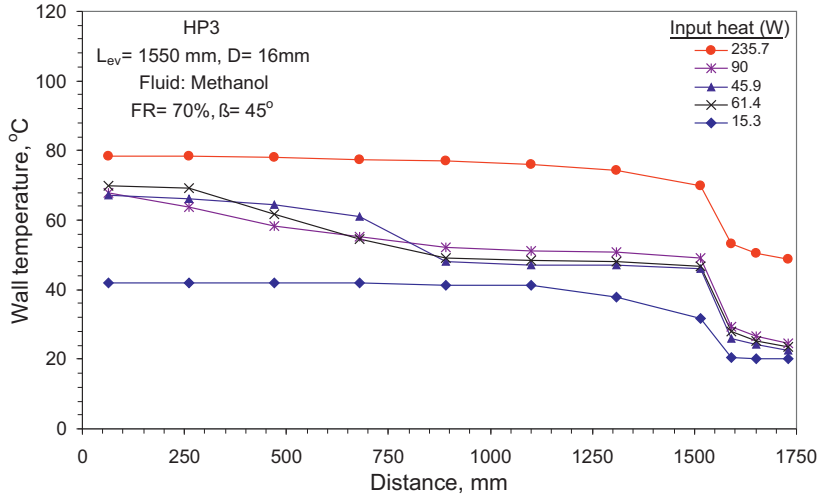

Figure 9: Evidence of Geyser phenomenon with methanol at 70% fill charge ratio.

phenomenon may be caused by a large lump of the working fluid that is forced upwards rapidly towards the condenser section, by a large expanding vapor bubble or a mass of multiple bubbles, causing the vapor existing inside the condenser section to be compressed and condensed within an instant of time. It is thought that the sudden bang (that may be considered as a kind of water hammer or steam hammer phenomena [6]) is originated by the instantaneous vapor compression inside the condenser section and the collapse of the uprising vapor bubble. Such a phenomenon was reported by Casarosa *et al.* [23], and was also observed by others [4,13,24,25] and was referred to as geyser phenomenon. This phenomenon disappeared as the input heat increased beyond the abovementioned range, where the noisy shocks vanished and the heat pipe operation became stable again. This phenomenon is too dangerous for it's damaging effect to the heat pipe. Therefore, fill charge ratios of 70% and 90% of the working fluids are not recommended for solar applications.

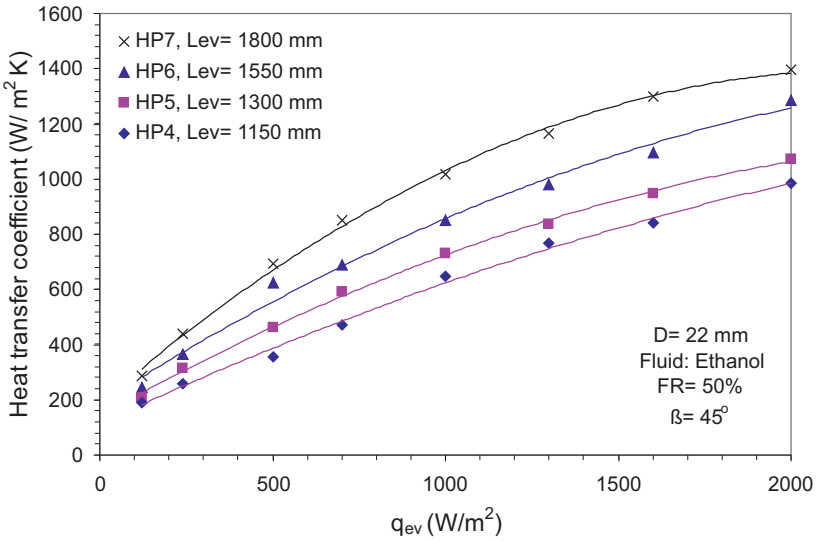

Figure 10: Effect of the heat pipe evaporator length (at 22 mm diameter) on the evaporator heat transfer coefficient at various heat flux inputs.

Figures 10 to 14 illustrate typical results for varying heat pipe evaporator length, diameter, working fluid, inclination angle and fill charge ratio on the average heat transfer coefficient. A significant increase in the heat transfer coefficient is observed with increasing heat flux and increased evaporator

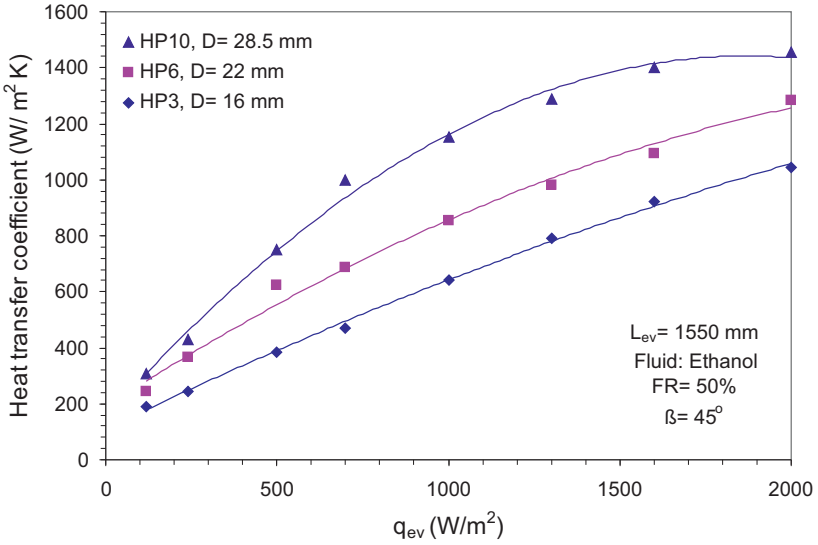

Figure 11: Effect of the heat pipe diameter (at 1550 mm evaporator length) on the evaporator heat transfer coefficient.

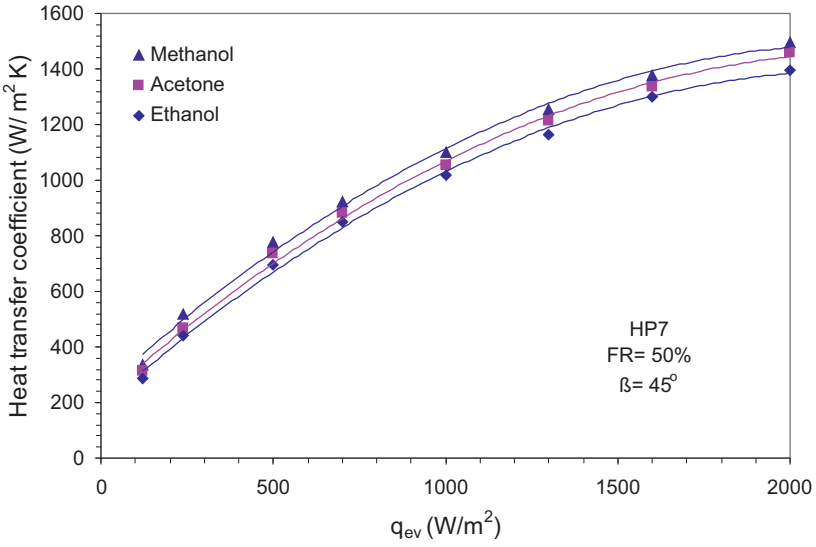

Figure 12: Effect of the working fluid type on the evaporator heat transfer coefficient at various heat flux inputs.

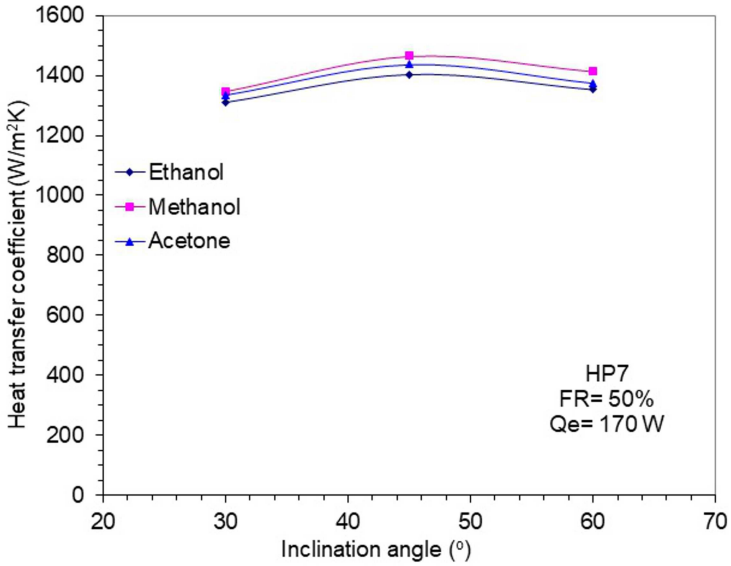

Figure 13: Effect of the inclination angle on the evaporator heat transfer coefficient with different working fluid.

length and diameter due to lower thermal resistance. Increased evaporator length from 1150 mm to 1800 mm increased the evaporator average heat transfer coefficient by a range from 8% to 32.3% (Fig. 10), while increasing the pipe diameter improved the evaporator average heat transfer coefficient by 4.7% to 50.8% to a value of 1454 W/(m^{2}K) (Fig. 11), depending on the input heat flux. The evaporator average heat transfer coefficient for methanol charged heat pipes (Fig. 12) is slightly larger than those with ethanol and acetone charged heat pipes at all inclinations by about 3–5%. This is due to the working fluids physical properties that operate at different amounts of superheat ($\Delta T_{ev} = T_{ev} - T_v$). The results in Fig. 13 show that 45° is the optimum inclination for maximum heat transfer coefficients and minimum operating temperature. This is true for all experimental heat pipes. This inclination angle is also suitable for solar application for being a good winter tilt angle in Baghdad (latitude: 33.3°N). The evaporator average heat transfer coefficient increases with increasing fill charge ratio, especially at higher heat fluxes, as shown in Fig. 14. A decrease was noticed with the three fluids at fill charges of 70% and 90%, which is thought to be due to the geyser effect as was discussed earlier.

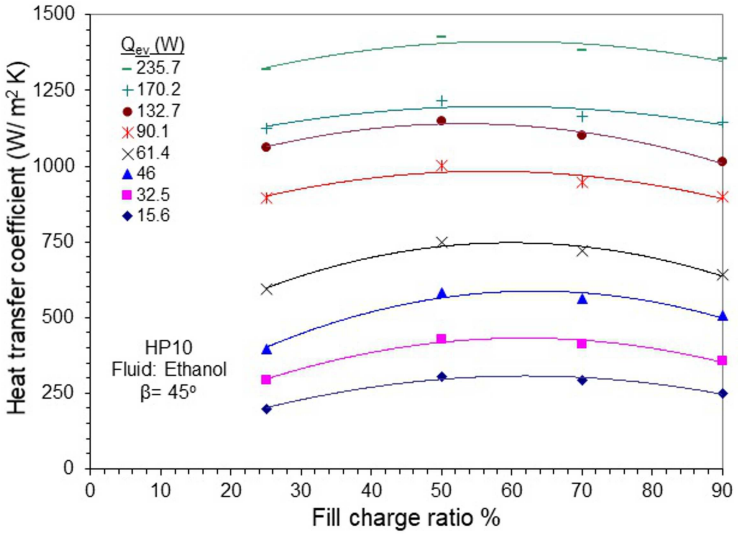

Figure 14: Effect of the working fluid inventory on the evaporator average heat transfer coefficient at various heat inputs.

Experimental results reveal that gravity-assisted wickless heat pipes (thermosyphons) can be satisfactorily used as thermal conductors in the solar applications. The experimental performance data were correlated in the following form:

$$\mathrm{Nu} = f(\mathrm{Re}_m, \mathrm{Gr}) \ , \tag{10}$$

where Re_m is a modified Reynolds number, obtained by multiplying the Reynolds number by the dimensionless aspect ratio L_{ev}/d which describes the contribution of the evaporator length and diameter on the heat transfer process. This dimensionless ratio is incorporated in the Reynolds number where the velocity and characteristic length dimensions play a dominant role. A possible form of Eq. (8) is a power law which has proved to be very useful in a variety of heat transfer applications. The final correlations for ethanol, methanol, and acetone are in the following forms with uncertainties of ±21%, ±20%, and ±22%, respectively (as shown in Figs. 15 to 17):

$$\mathrm{Nu}_{corr} = 0.508\mathrm{Re}^{0.2671}(L_{ev}/d_i)^{0.2671}\mathrm{Gr}0.2053 \ , \tag{11}$$

$$\mathrm{Nu}_{corr} = 0.0073\mathrm{Re}^{0.505}(L_{ev}/d_i)^{0.505}\mathrm{Gr}^{0.2091} \ , \tag{12}$$

$$\mathrm{Nu}_{corr} = 0.0323\mathrm{Re}^{0.2113}(L_{ev}/d_i)^{0.2113}\mathrm{Gr}^{0.2126} \ . \tag{13}$$

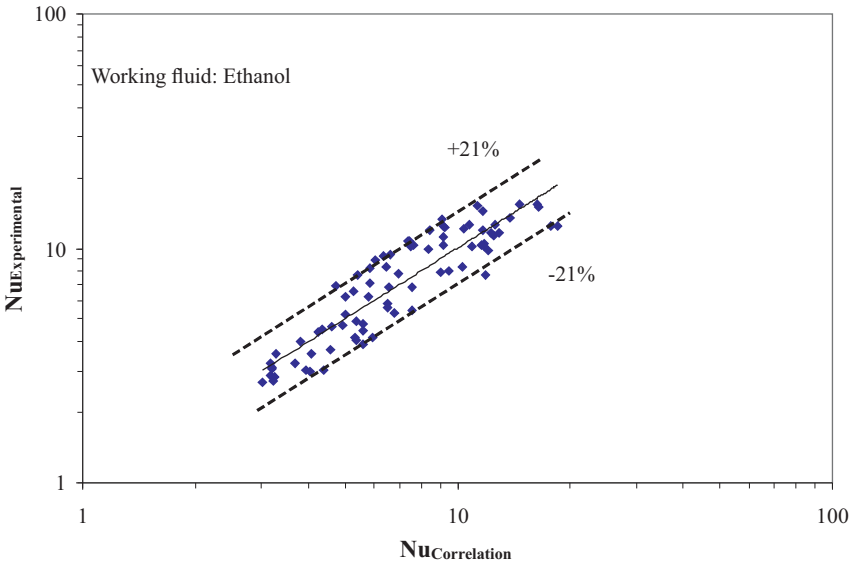

Figure 15: Data correlation of 50% ethanol charged heat pipes.

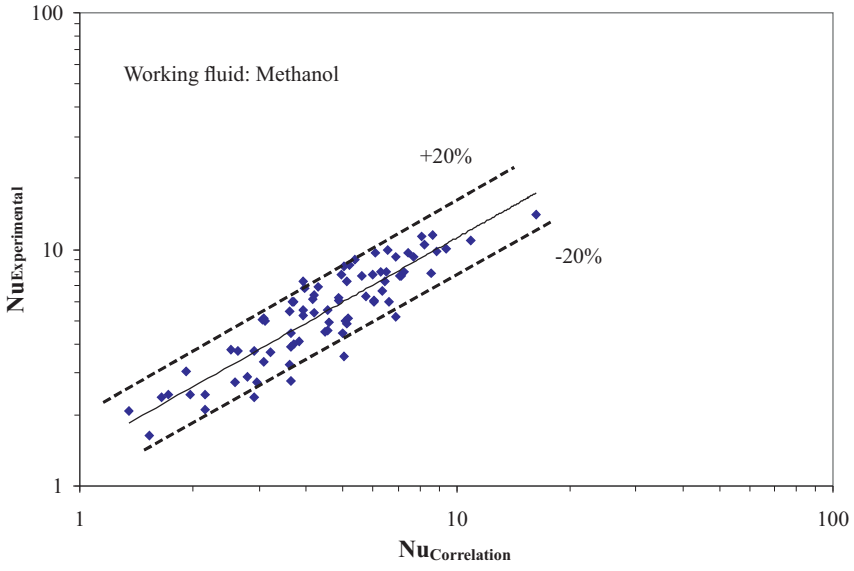

Figure 16: Data correlation of 50% methanol charged heat pipes.

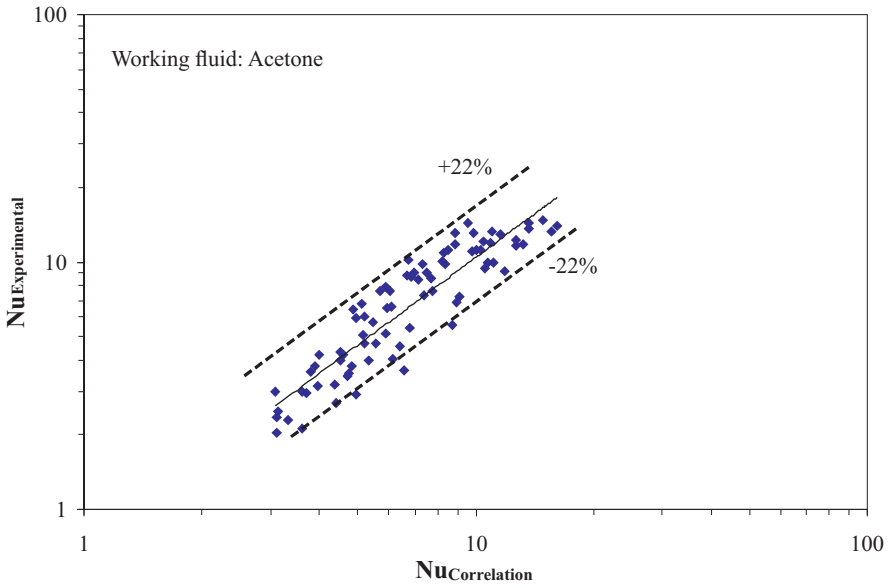

Figure 17: Data correlation of 50% acetone charged heat pipes.

5 Conclusions

1. Increasing the evaporator length and diameter increased the heat pipe operating temperature and the evaporator heat transfer coefficient with slight differences between the three working fluids.
2. Reduced evaporator temperatures and maximized heat transfer coefficients are obtained at an optimum inclination angle of 45°.
3. Increasing the fill charge ratio decreased the operating temperature and improved the heat transfer coefficient to maximum values at 50% fill charge for all heat pipes and working fluids.
4. The geyser phenomenon was observed with the three fluids at heat inputs of 40–110 W (230–1900 W/m^2) for all heat pipes at 70% and 90% fill charge ratios.
5. Gravity-assisted wickless heat pipes (thermosyphons) can be satisfactorily used as thermal conductors in the solar applications.

Received 22 December 2018

References

[1] Jiao B., Qiu L., Zhang X., Zhang Y.: *Investigation of the effect of filling ratio on the steady-state heat transfer performance of a vertical two-phase closed thermosyphon.* Appl. Therm. Eng. **28**(2008), 11, 1417–1426.

[2] Larkin B.S.: *An experimental investigation of a low heat flux, wickless heat pipe.* Trans. Canadian Soc. Mech. Eng. **7**(1983), 2, 96–99.

[3] Dristoiu D., Ristoiu T., Cosma C., Cenan D.: *Experimental investigation of inclination angle on heat transfer characteristics of closed two-phase thermosyphon.* In. Proc. 5th General Conf. Balkan Physical Union, Aug., 2003.

[4] Shiraishi M. Nakano A. Terdtoon P. , Murakami M.: *Performance limits of inclined gravity assisted heat pipe.* In: Proc. 10th Int. Heat Pipe Conf., H2-9, Sep. 21–25, 1997.

[5] Shiraishi M., Kim Y., Murakami M., Terdtoon P.: *A correlation for the heat transfer rate in an inclined two- phase closed thermosyphon.* In: Proc. 5th Int. Heat Pipe Symp., Melbourne, 1996.

[6] Negishi N., Sawada T.: *Heat transfer performance of inclined two- phase closed thermosyphon.* Int. J. Heat Mass Transf. **26**(1983), 8, 1207–1213.

[7] Mahdy M.: *Experimental Investigation of Low Heat Flux Heat Pipes with and without Adiabatic Section for Solar Application.* PhD thesis, University of Baghdad, Baghdad 2005.

[8] Kayansayn N.: *The gravity assisted heat pipe with application to concrete shell steam condensers.* J. Heat Recov. Sys. CHP **6**(1986), 5, 389–397.

[9] Hussein H., El-Ghetany H., Nada S.: *Performance of wickless heat pipe flat plate solar collectors having different pipe cross section geometries and filling ratios.* Energy Convers. Manage. **47**(2006), 11-12, 1539–1549.

[10] El-Nasr M., El-Haggar S.: *Performance of a wickless heat pipe solar collector.* J. Energy Sourc. **15**(1993), 3, 513–522.

[11] Hussein H.: *Theoretical and Experimental Investigation of a Wickless Heat Pipe Flat Plate Solar Collector.* PhD thesis, Faculty of Engineering, Cairo University, Cairo 1997.

[12] Murgu Z., Murgu D., Cojocaru L., Huzum M., Tvardochlieb E.: *Heat pipes for sun energy conversion.* In: Proc. 3rd Int. Heat Pipe Conf., Palo Alto, 1978.

[13] Witwit A.M.: *A Study of The Gravity Assisted and Variable Conductance Heat Pipes With an Internal Wall Separating Liquid and Vapor Phases.* PhD thesis. Mech. Eng. Dept., University of Baghdad, Baghdad 1998.

[14] Hahne E., Gross U.: *The Influence of The Inclination Angle on the Performance of a Closed Two Phase Thermosyphon.* In: Advances in Heat Pipe Technology (D. Reay, Ed.), 1982, 125–136.

[15] El-Genk M., Saber H.: *Heat transfer correlations for small uniformly heated liquid pools.* Int. J. Heat Mass Transf. **41**(1998), 2, 261–274 .

[16] El-Genk M., Saber H.: *Heat transfer in the evaporator of closed two phase thermosyphons.* In: Proc. 10th Int. Heat Pipe Conf. X-10 Sep. 21–25, 1997.

[17] Imura H., Kusuda H., Ogata T., Miyazki T., Sakamoto N.: *Heat transfer in two phase closed type thermosyphons.* J. Heat Tran. Jap. Res. **8**(1979), 2, 41–53.

[18] Imura H., Kusuda H., Ogata J., Miyazaki T., Sakamoto N.: *Heat transfer in two-phase closed type thermosyphon.* Trans. JSME B **45**(1979), 393, 712–722.

[19] Kaminaga F., Hashimoto H., Feroz M., Goto K., Masumura K.: *Heat transfer characteristics of evaporation and condensation in a two-phase closed thermosyphon.* In: Proc. 10th Int. Heat Pipe Conf. H-1-6, Sep. 21–25, 1997.

[20] Noie S.H.: *Heat transfer characteristics of a two-phase closed thermosyphon.* Appl. Therm. Eng. **25**(2005), 495–506.

[21] Jialun H., Ma Tongze M., Zhengfang Z.: *Investigation of boiling liquid pool height of a two phase closed thermosyphon.* In: Proc. 8th Int. Heat Pipe Conf., 1992, 154–159.

[22] Sayegh A. Danielewicz J., Tomczak W.: *Thermal performance of low density heat transfer in two phase closed thermosyphon.* In: proc. 10th Int. Heat Pipe Conf., H-2-8, Stuttgart, Sep. 21–25, 1997.

[23] Casarosa A., Latrofa E., Shelginski A.: *The geyser effect in a two- phase thermosyphon.* Int. J. Heat Mass Transf. **26**(1983), 6, 933–941.

[24] Bezrodney M., Elekseyenko D.: *Boiling heat transfer in closed two phase thermosyphon.* Heat Transfer-Soviet Res. **9**(1977), 5, 14–19.

[25] Imura H., Ipposhi S., Sakamoto M.: *Experimental investigation of critical heat flux in two phase closed thermosyphon.* In: Proc. 10th Int. Heat Pipe Conf., H-2-7, Stuttgart, Sep. 21–25, 1997.